Improving transmittance of long-wave infrared guided-mode resonant filters

Neelam Gupta[a,*] **and Junyeob Song**[b]
[a]DEVCOM Army Research Laboratory, Adelphi, Maryland, United States
[b]University of Delaware, Department of Electrical and Computer Engineering, Newark, Delaware, United States

Abstract. The long-wave infrared (LWIR) spectral region spanning from 8 to 12 μm is useful for many scientific and industrial applications. Many of these applications require use of either a bandpass or a bandstop filter that can be realized by the guided-mode resonance (GMR) effect with subwavelength periodic features in layered dielectric materials transparent in the LWIR. The GMR filters operating in the LWIR region are fabricated by depositing an amorphous germanium (Ge) film to form a zero-contrast (ZC) waveguide-grating (WGG) on a polished zinc selenide (ZnSe) substrate. In general, the backside of a ZnSe substrate with refractive index 2.41 is uncoated causing a 17% Fresnel-reflection loss in the light transmitted through the filter due to a large impedance mismatch at the ZnSe/air interface. Because we use such filters in the LWIR laser experiments for notch filtering, to improve the filter transmittance we used ZnSe substrates coated on one-side with broadband antireflection coating (ARC) covering the 7 to 12 μm spectral range to fabricate GMRFs with one-dimensional (1D) Ge ZC WGG. We employed high-spatial resolution e-beam lithography and reactive-ion etching nanofabrication techniques to achieve high-performance large-area (12×12 mm^2) 1D notch filters with subwavelength periods. We characterized polarization dependent spectral performance of the prototype filters with both coherent and incoherent incident light using a tunable quantum cascade laser system that spans the 7 to 12 μm region, and a Fourier transform infrared spectrometer with collimated incident beam to achieve close to 15% improvement in the peak transmittance as well as significant reduction in coherent noise compared to our earlier results with GMRFs without ARC. Here, we present the filter design simulation and measurement results. [DOI: 10.1117/1.OE.62.3.035102]

Keywords: guided-mode-resonance; longwave infrared; notch filters; germanium; zinc selenide; flat substrate; wedged substrate; subwavelength; gratings; quantum cascade laser; collimated FTIR; rigorous coupled-wave analysis; polarization dependence; antireflection coating; Fabry-Perot resonance.

Paper 20221030G received Sep. 19, 2022; accepted for publication Feb. 14, 2023; published online Mar. 19, 2023.

1 Introduction

The 8- to 12-μm LWIR spectral region corresponds to an atmospheric window as well as to the peak terrestrial emission and is widely used for day/night sensing and imaging applications. Some of these applications require use of compact spectrally tunable notch or bandstop filters, which reflect a narrow band of incident light while transmitting the rest. Such filters cannot be fabricated using traditional multilayer thin film technology used at shorter wavelengths due to impractical time required for fabrication in the LWIR range. In 1992, Magnusson and Wang[1] showed that small compact notch filters can be designed based on the guided-mode resonance (GMR) effect in dielectric WGG and since then such filters have been demonstrated from the visible to the LWIR spectral regions.[1–16] A GMR filter (GMRF) based on one-dimensional (1D) gratings only on one side of the substrate is polarization sensitive,[1–10] whereas GMRFs based on

*Address all correspondence to Neelam Gupta, neelam.gupta.civ@army.mil

two-dimensional gratings are polarization insensitive at normal incidence and polarization sensitive at non-normal incidence.[12–15] Recently, we demonstrated polarization insensitivity at normal incidence for a double-sided LWIR GMRF with orthogonal 1D gratings on either side of a substrate,[11] as well as a combination of two separate 1D LWIR GMRFs with linear gratings in orthogonal orientations.[9] Our previous work on 1D LWIR GMRFs used flat ZnSe substrates without any ARC.[7,9–11] In the present work, we fabricated and characterized 1-D GMRFs on two different types of substrates with ARC to reduce coherent noise and increase transmittance.

In our earlier work, we measured spectral transmittance from 8 to 12 μm using a quantum cascade laser (QCL) system for the 1D LWIR GMRFs on flat ZnSe substrates without any ARC applied on the backside. Both the simulated and measured spectra had a lot of high-frequency Fabry-Perot (FP) resonance noise arising due to reflections of coherent light from the parallel facets of the substrate with a peak transmittance ~78%.[7,10] We also investigated use of several alternate thin layers of Ge and ZnSe on the substrate to act as a broadband ARC and got only marginal improvement even with eight layers.[7] To overcome these issues, we decided to use two different kinds of commercial ZnSe substrates—flat and wedged with a broadband ARC applied on the backside to get higher transmittance and lower coherent noise. The reason for using a wedged substrate was to eliminate the FP resonance in the substrate without parallel facets. In addition, since our earlier GMRF characterization at non-normal incidence of light was limited to only a single polarization defined by the QCL,[7,10] we also used a modified commercial FTIR with a collimated incident beam to measure transmittance with both incident polarizations of light.[11,14] In this paper, we present transmittance measurements for 1D GMRFs with ARC on both the flat and wedged substrates taken with the QCL as well as the FTIR for normal as well as non-normal incidence of light for both polarizations. To the best of our knowledge, this is the first time such transmittance measurements for the 1D LWIR GMRFs with ARC are reported.

We designed and fabricated 1D ZC subwavelength WGG GMR notch filters operating from 7 to 12 μm using high-refractive index (n) transparent dielectric materials, i.e., an amorphous Ge film with $n = 4.1$ on a ZnSe substrate with $n = 2.41$. The ZC WGG is composed of a grating on the sublayer waveguide guiding lateral Bloch modes coupled by evanescent diffraction orders.[1–4] Due to the leaky mode excitation in the periodic WGG, the notch filtering response occurs, reflecting a narrow spectral band of the polarized incident light while transmitting the rest. At the normal incidence, the 1D filter reflects the incident broadband light at a single narrowband notch for each polarization while transmitting the rest. At non-normal incidence, such filters reflect at two narrow spectral bands for each polarization while transmitting the rest of the incident light. When the incident light polarization direction is parallel to the linear grating, it is considered the transverse electric (TE); when it is perpendicular to the grating, it is labeled the transverse magnetic (TM) polarization. The notch wavelength(s) for both normal and non-normal incidence are polarization sensitive. During the measurement, we change the angle of incidence of light by mechanically tilting the filter.[7,10]

We carefully chose the device parameters—grating period, fill factor, grating thickness, and waveguide thickness for this spectral range of operation for a Ge ZC WGG on a ZnSe substrate. We implemented the rigorous coupled-wave analysis (RCWA) algorithm to carry out the modeling and design of the filters to obtain the best spectral transmittance.[17] To approximate the commercial proprietary broadband ARC in our RCWA simulations, we used a four-layer structure on the backside of ZnSe substrate.[16,18] Physical vapor deposition, e-beam lithography, and reactive-ion etching (RIE) techniques were used to deposit and fabricate high-spatial resolution high-quality 1D prototype GMRFs on both flat and wedged commercial substrates with ARC applied on one-side. As mentioned earlier, we characterized the polarization dependent filtering performance of such filters using two separate experimental setups using coherent and incoherent incident light—(i) an automated room-temperature QCL system tunable from 7 to 12 μm and a thermal detector, and (ii) a modified commercial FTIR spectrometer with a collimated incident beam and a high-sensitivity, high-speed liquid nitrogen (LN_2) cooled mercury cadmium telluride (MCT) detector at both normal and non-normal incidence of light. We attained an excellent agreement between the theoretical and experimental results.

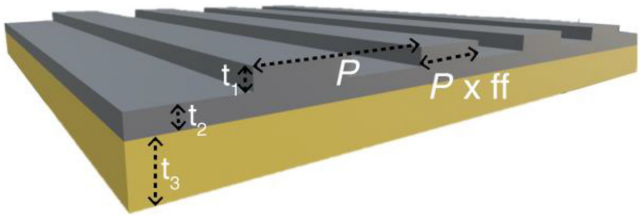

Fig. 1 Schematic drawings of a 1D GMRF with parameter labels. Gray and yellow colors represent Ge and ZnSe, respectively.

2 Materials and Methods

2.1 *Modeling and Simulation*

To predict the wideband electromagnetic properties of the 1D GMRFs, we implemented the RCWA to obtain the design parameters using Ge and ZnSe.[17] In our model, the input parameters are refractive indices of incident and exit regions, grating layer, waveguide (WG) layer, and the substrate; incidence angle; period (P), thickness (t_1), and fill factor (ff) of the grating; thickness of the planar WG (t_2); and thickness of the substrate (t_3) as schematically shown in Fig. 1 representing a 1D metamaterial filter.

We chose design parameter values for the GMRF on the flat substrate by scanning over the parameter values to obtain the highest diffraction efficiency—P = 2.9 μm; ff = 0.35; t_1 = 500 nm; t_2 = 1.0 μm, with t_3 = 1 mm such that they correspond to the 7 to 12 μm range of filtering operation. With subwavelength parameter values, only the zero-order transmittance ($\mathbf{T_0}$) contributes to GMR as all other orders are evanescent. In Figs. 2(a)–2(d) for the TE, we show computed contour color maps that display the spectral transmittance over 7 to 12 μm as a function of P, ff, t_1, and t_2 assuming an infinite thickness of the substrate with a color bar for $\mathbf{T_0}$ showing values from 0 to 1 included on the right-hand side, and in Figs. 2(e)–2(h) for the TM polarization. The blue color corresponds to low transmittance value and the red color is for high transmittance. When the corresponding transmittance spectra are plotted, the blue regions correspond to the notch wavelengths. These plots show that for each polarization in Figs. 2(a) and 2(e) as P increases (ff, t_1, and t_2 fixed) the notch wavelength increases linearly; Figs. 2(b) and 2(f) show that change in ff (P, t_1, and t_2 fixed) does not affect value of the notch wavelength much but the full width at half maximum (FWHM) changes; similarly Figs. 2(c) and 2(g) show change in t_1 (P, ff, and t_2 fixed) does not change value of the notch wavelength much but changes value of the FWHM; Figs. 2(d) and 2(h) show change in t_2 (P, ff, and t_1 fixed) changes the notch wavelength significantly in a nonlinear manner. We drew dashed lines on each color plot corresponding to the design value of the parameter that is varied and for the TE polarization in each case we obtained notch wavelength close to 9.8 μm and for the TM it is 8.4 μm. In Figs. 3(a) and 3(b), we include the color plot of spectral transmittance for each polarization as a function of the angle of incidence (P, ff, t_1, and t_2 fixed) to show polarization dependent spectral tuning over 7 to 12 μm with a $\mathbf{T_0}$ color bar included on the right-hand side. These plots show that for each polarization there is one notch wavelength at normal and two notches for non-normal incidence.

2.2 *Device Fabrication and Simulation*

We fabricated 1D GMRF on two different types of commercial ZnSe substrate (25.4 mm diameter, 1 mm thick) with an ARC on the backside to improve transmittance and to see which one yields less noisy spectra when used with lasers. The two different substrates were—(i) flat with ARC on one-side (Crystran Limited, United Kingdom) and (ii) with 0.5 deg wedge and the ARC applied on the wedge side (Thorlabs Inc., United States). For the fabrication of an ebeam-written 1D GMRF, we followed the procedure as described in detail in our earlier papers.[10,11] The main difference is that since the one side of the ZnSe substrate is coated with a broadband ARC covering 7 to 12 μm, to protect the ARC side of the substrate, we first spin coated it with polymethylmethacrylate (PMMA) at 3000 RPM and baked it at 180°C for 10 min and then proceeded with depositing a Ge ZC WGG on the uncoated side of the ZnSe substrate using the e-beam

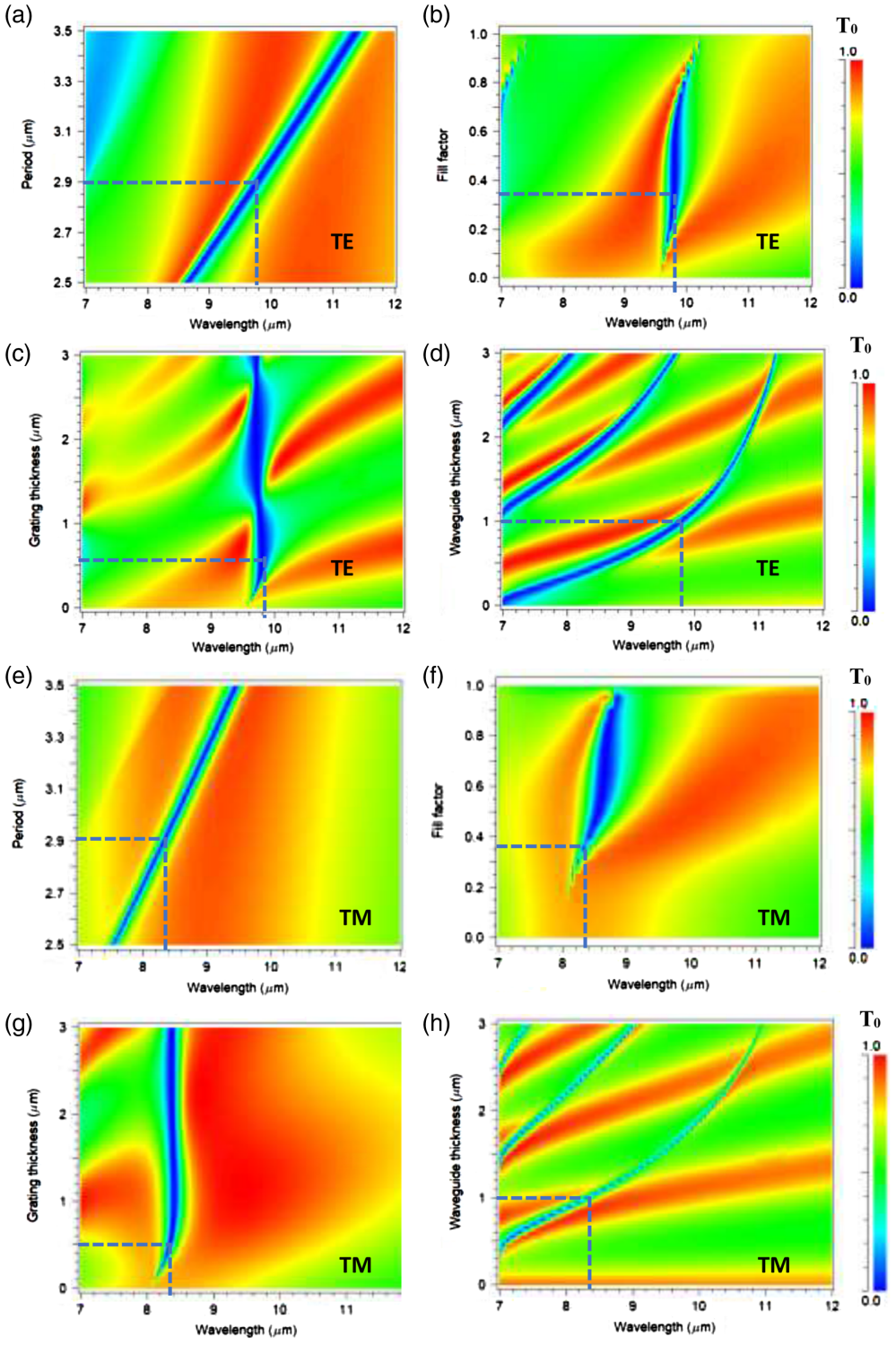

Fig. 2 Color plots of spectral transmittance for a 1D GMRF at normal incidence of light over 7 to 12 μm with a color bar on the right-hand side as a function of P, ff, t_1, and t_2, respectively with $t_3 = \infty$ for both TE and TM incident polarizations. Spectral transmittance as a function of P (ff $= 0.35$, $t_1 = 500$ nm, $t_2 = 1\mu$m) for (a) TE and (e) TM; as a function of ff ($P = 2.9$ μm, $t_1 = 500$ nm, $t_2 = 1$ μm) for (b) TE and (f) TM; as a function of t_1 ($P = 2.9$ μm, ff $= 0.35$, $t_2 = 1$ μm) for (c) TE and (g) TM; and as a function of t_2 ($P = 2.9$ μm, ff $= 0.35$, $t_1 = 500$ nm) for (d) TE and (h) TM polarization. Dashed lines are drawn corresponding to the design values of these parameters.

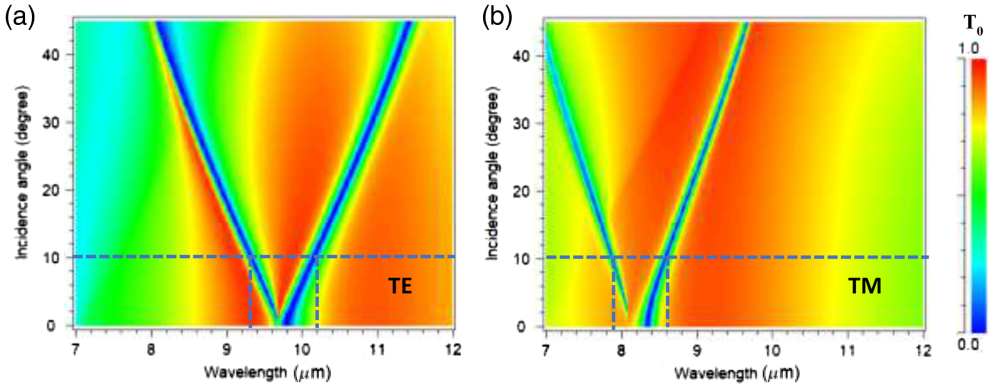

Fig. 3 Color plots of spectral transmittance with a color bar on the right-hand side for a 1D GMRF as a function of angle of incidence over 7 to 12 μm spectral interval for incident (a) TE and (b) TM polarized light with $P = 2.9$ μm, ff $= 0.35$, $t_1 = 500$ nm, $t_2 = 1.0$ μm and with $t_3 = \infty$. This shows spectral tuning can be achieved by changing the angle of incidence for each polarization. Dashed lines are drawn corresponding to 5 deg angle of incidence.

lithography and RIE, by following the steps listed in Ref. 10. Afterward to complete the fabrication process, PMMA layer is removed[11] yielding a fabricated filter. The grating period, thickness, and fill factor for a fabricated GMRF are measured using atomic force microscopy (AFM) and scanning electron microscopy (SEM) images of the device. These parameter values depend on both the e-beam lithography and the RIE process.

For a fabricated filter on a flat substrate, we include the AFM and SEM images in Fig. 4 that yield the parameter values—$P = 2.91$ μm, ff $= 0.36$, $t_1 = 518$ nm, and $t_2 = 1.015$ μm that are close to the design values drawn as dashed lines in Fig. 2, clearly showing the corresponding notch wavelengths. In Fig. 5, we show the simulated transmittance spectra using RCWA for both the TE and TM polarization at different angles of incidence of light with the measured values of the flat substrate filter parameters. We used the measured value $n = 4.1$ using an LWIR ellipsometer for a thin film of e-beam-grown amorphous Ge on a ZnSe substrate. We approximated the commercial broadband ARC using the following layers at the backside of the 1-mm-thick substrate—677-nm-thick zinc sulfide (ZnS, $n = 2.25$), 56-nm-thick Ge, 72-nm-thick ZnS, and 1.68-μm-thick yttrium fluoride (YF_3, $n = 1.5$).[16,18] This ARC worked quite well for incident coherent light from 7.3 to 12 μm in reducing FP noise as compared to substrate without ARC[7,10] but did not work below 7.3 μm. These simulations are shown for both the TE and TM polarizations at 0 deg and 5 deg incidence in Fig. 5(a) to be compared with the QCL measurements. By comparing the simulated spectra for GMRFs without ARC included in

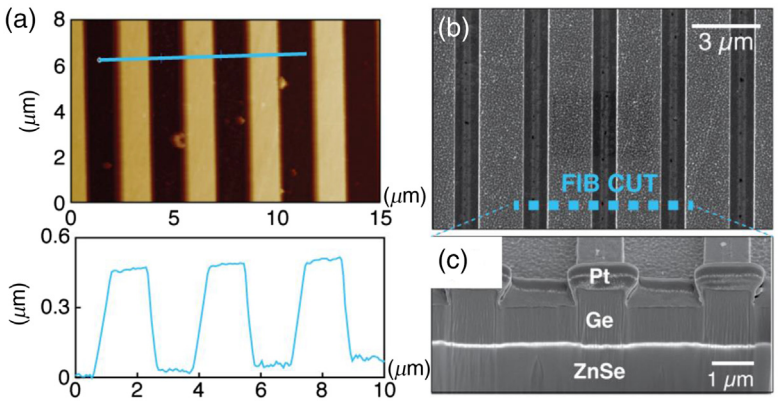

Fig. 4 (a) AFM and (b) and (c) SEM images of 1D GMRF. Focused ion-beam (FIB) milling was carried out by depositing a platinum layer on top to show detailed shape of the grating structures and to confirm that the grating sidewalls are straight.

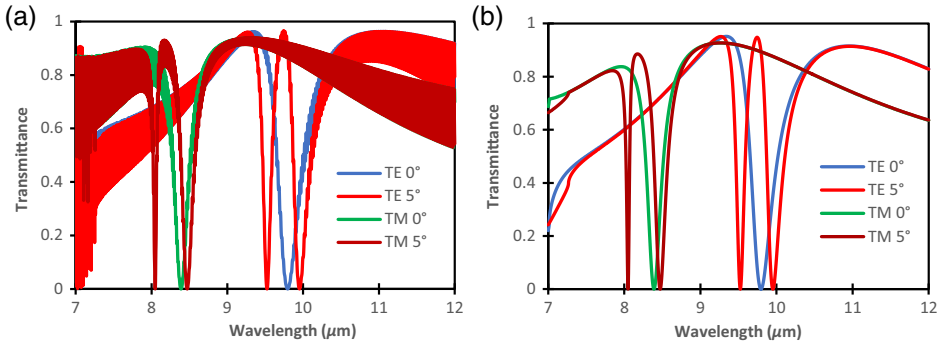

Fig. 5 Simulated spectral transmittance of 1D GMRF fabricated on a flat substrate for both the TE and TM incident polarizations at incident angles of 0 deg and 5 deg for (a) with ARC on the backside of the substrate and (b) assuming an infinite thickness for the substrate corresponding to a perfect ARC on the backside of the substrate as well as to incoherent light transmission.

Refs. 7 and 10 to Fig. 5(a), we can see that simulated ARC reduces FP noise considerably. We also carried out simulations assuming the substrate thickness to be infinite (corresponding to a perfect ARC on the backside of the substrate as well as to incoherent light transmission) for both polarizations at 0 deg and 5 deg incidence and present them in Fig. 5(b) for comparison with the modified FTIR measurements. At normal incidence, there is a single notch at 9.8 μm for the TE and at 8.4 μm for the TM polarization. For 5 deg angle of incidence there are two notches at 9.52 and 9.95 μm for the TE and at 8.05 and 8.47 μm for the TM polarization. The maximum transmittance from all these simulations is ~93% while the peak simulated transmittance obtained with GMRFs without ARC was around 78%.[7,10]

For the wedged substrate GMRF, different design values of parameters were used than for the flat substrate, and the measured values of these parameters are—$P = 3.1$ μm, ff $= 0.35$, $t_1 = 357$ nm, and $t_2 = 1.393$ μm. Alignment is a major issue in e-beam lithography of the wedged substrate due to the 0.5 deg-prism structure. Also, it is not possible to model the wedged GMRF using RCWA due to the non-periodicity of the wedge. Due to the difference in the filter parameter values from the flat substrate to wedged substrate GMRFs, the notch wavelengths are expected to be different for the two types of filters.

3 Measurement and Discussion

Since these filters will be used in both laser and incoherent light experiments, we characterized the filters transmittance using two separate experimental setups—(i) an automated QCL (Daylight Solutions model 2300) and uncooled broadband thermopile 16-mm-diameter detector power meter (Ophir-Spiricon model Vega-B power meter with a 10A-PPS detector) over the spectral range from 7 to 12 μm where the laser is vertically polarized and transmittance is directly measured using coherent light; and (ii) a modified commercial FTIR (Bruker 70) spectrometer with a collimated incident beam (a traditional FTIR spectrometer could not be used as the incident beam on the sample is focused and does not meet plane wave incidence requirement to correspond to the RCWA simulations), a high-sensitivity LN_2-cooled 1-mm-diameter MCT detector with 20 kHz scan speed for incoherent light measurements, and an LWIR wire grid polarizer installed before the sample to change the incident light polarization. Both these experimental setups have been described in detail in Ref. 11.

For the GMRFs with a flat substrate, we present the spectral transmittance measured by the QCL at 0 deg and 5 deg angles of incidence for the TE and at 0 deg for the TM polarization in Fig. 6(a), and in Fig. 6(b) the modified FTIR data for both polarizations at 0 deg and 5 deg incidence. As described in Ref. 10, with QCL we can measure transmittance spectra at various angles for the TE polarized light due to the vertical polarization of the laser but only at normal incidence for the TM polarization. With FTIR, we can measure transmittance for both polarizations at all angles of incidence of light. The notch values from the QCL measurements for TE are at 9.83 μm for 0 deg and at 9.51 and 10 μm for 5 deg; and for TM at 8.4 μm for 0 deg.

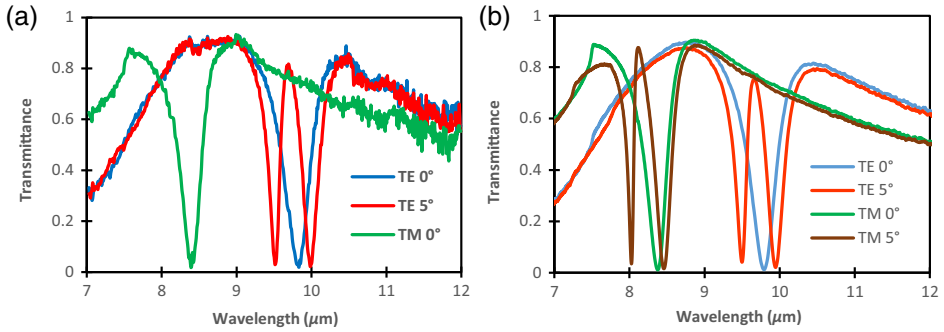

Fig. 6 Measured spectral transmittance of 1D GMRF fabricated on a flat substrate with ARC on the backside for both the TE and TM incident polarizations at incident angles of 0 deg and 5 deg using the (a) QCL (5 deg data for TE only) and (b) modified FTIR experimental setup.

The notch values from the FTIR measurements for TE are at 9.8 μm for 0 deg and at 9.5 and 9.95 μm for 5 deg; and for TM at 8.38 μm for 0 deg and at 8.0 and 8.46 μm for 5 deg. The measured notch wavelengths are close to the simulated values within experimental uncertainties. The measured maximum transmittance from the QCL measurements is ~93%, which is the same as predicted by the simulations while from the FTIR measurements; it is ~90%, which is slightly lower than the predicted values. The QCL-measured peak transmittance for GMRF without ARC was ~78%.[7,10] We should note that the QCL-measured spectra for GMRF with ARC has significantly lower noise in comparison to measured spectra in Refs. 7 and 10 for filters without ARC.

For the GMRF with wedged substrate, similar QCL data at 0 deg and 5 deg angles of incidence for the TE and at 0 deg for the TM polarization are included in Fig. 7(a) as we want to observe the effect of wedge in reducing the coherent light noise; and in Fig. 7(b) we show the collimated-FTIR data at 0 deg and 5 deg incidence. It is clear from comparison of Figs. 6(a) and 7(a) that the noise reduction in QCL data for the two types of GMRFs is similar and the wedge does not reduce the laser noise more. The notch values from the QCL measurements for TE are at 10.35 μm at 0 deg and at 10.06 and 10.51 μm for 5 deg; and for TM at 8.64 μm at 0 deg. The notch values from the FTIR measurements for TE are at 10.32 μm at 0 deg and at 10.05 and 10.45 μm for 5 deg; and for TM at 8.61 μm at 0 deg and at 8.3 and 8.7 μm for 5 deg. The QCL and FTIR measured notch wavelengths match within the experimental uncertainties. The measured notch wavelengths for the wedged substrate filter are different than for the flat substrate filter due to slight difference in values of P, t_1, and t_2 for the two types of fabricated filters. Also, comparison of Figs. 6(b) and 7(b) shows that 5 deg incidence measurement notches are not as deep for the wedged sample as for the flat one due to the alignment issues with the wedged filter for the smaller field of view of the MCT detector.

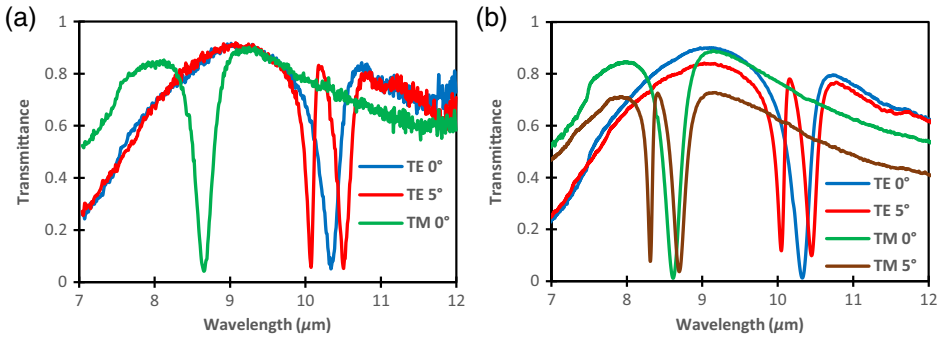

Fig. 7 Measured spectral transmittance of 1D GMRF fabricated on a wedged substrate with ARC on the backside for both the TE and TM incident polarizations at incident angles of 0 deg and 5 deg using the (a) QCL (5 deg data for TE only) and (b) modified FTIR experimental setup.

4 Summary and Conclusion

We used RCWA algorithm to design the GMR notch filters with the best transmittance values by scanning over the parameter values. With subwavelength parameter values, only the zero-order diffraction contributes to GMR as all other orders are evanescent. We designed and fabricated 1D ZC WGG GMRFs on ZnSe substrates that were flat as well as with a small wedge that had an ARC applied on the backside to see if the filter transmission can be improved and coherent noise can be reduced. We used a four-layer ARC structure[16,18] to approximate the commercial 7- to 12-μm broadband ARC applied on the backside of the ZnSe substrates. We used a room-temperature tunable QCL system to carry out direct transmittance measurement as well as a modified FTIR spectrometer to carry out filter transmittance measurements at both normal and non-normal incidence of light for both polarizations. We observed expected transmittance improvement as predicted by theory with maximum transmittance ~93% for GMRF with ARC, which is ~15% higher than GMRFs without ARC used in our earlier work.[7,10] The ARC on the backside of the substrate significantly reduced the FP reflection noise in the substrate as compared to no ARC in our previous work.[7,10] Based on our results we conclude there is no advantage in using a substrate with small wedge with ARC as compared to a flat substrate with ARC on the backside as the reduction in coherent light noise is comparable for either substrate. This is noteworthy as fabrication of a GMRF on a wedged substrate requires careful alignment of gratings relative to the wedge orientation as well as such GMRFs need to be oriented properly in an experimental setup.

As predicted, the 1D GMRFs are polarization-dependent, and our results clearly illustrate this dependence. We observed that there is a single notch at normal incidence and two notches at non-normal incidence for each polarization. This implies that the notch wavelength changes as the angle of incidence of light changes, facilitating spectral tunability of 1D GMRFs, which is useful when used with sources with different emission wavelengths. In other words, the notch wavelength of the filter can be tuned by mechanically tilting the filter to change the angle of incidence. Based on close agreement between the theoretical and experimental spectral transmittance for the fabricated GMRFs, it is clear that 1D GMRF on a flat substrate with ARC transmits more light than without ARC and it is useful for polarization dependent tunable notch filtering.

Acknowledgments

DEVCOM Army Research Laboratory (Grant No. W911NF-18-2-0217).

References

1. R. Magnusson and S. S. Wang, "New principle for optical filters," *Appl. Phys. Lett.* **61**, 1022 (1992).
2. R. Magnusson, "Wideband reflectors with zero-contrast gratings," *Opt. Lett.* **39**, 4337–4340 (2014).
3. S. S. Wang and R. Magnusson, "Multilayer waveguide-grating filters," *Appl. Opt.* **34**, 2414–2420 (1995).
4. D. Rosenblatt, A. Sharon, and A. A. Friesem, "Resonant grating waveguide structures," *IEEE J. Quantum Electron.* **33**, 2038 (1997).
5. J.-N. Liu et al., "Optimally designed narrowband guided-mode resonance reflectance filters for mid-infrared spectroscopy," *Opt. Express* **19**, 24182–24197 (2011).
6. B. Hogan et al., "Realization of high-contrast gratings operating at 10 μm," *Opt. Lett.* **41**, 5130–5133 (2016).
7. N. Gupta and M. S. Mirotznik, "Performance characterization of tunable longwave infrared notch filters using quantum cascade lasers," *Opt. Eng.* **57**, 127101 (2018).
8. D. J. Carney and R. Magnusson, "Fabrication methods for infrared resonant devices," *Opt. Lett.* **43**, 5198–5201 (2018).
9. K. J. Lee et al., "Unpolarized resonant notch filters for the 8–12 μm spectral region," *Opt. Lett.* **45**, 4452–4455 (2020).

10. N. Gupta and J. Song, "High-quality large-scale electron-beam-written resonant filters for the long-wave infrared region," *Opt. Lett.* **46**, 348–351 (2021).
11. N. Gupta and J. Song, "Longwave infrared polarization independent Monolithic guided-mode resonance filters with double-sided orthogonal linear gratings," *Opt. Contin.* **1**(4), 674–683 (2022).
12. Y. Zhong et al., "Mid-wave infrared narrow bandwidth guided mode resonance notch filter," *Opt. Lett.* **42**, 223–226 (2017).
13. A. S. Lal Krishna et al., "Polarization-independent angle-tolerant mid-infrared spectral resonance using amorphous germanium high contrast gratings for notch filtering application," *OSA Contin.* **3**, 1194–1203 (2020).
14. N. Gupta and J. Song, "Polarization independent electron-beam written 2-D longwave infrared guided-mode resonant filters," *Opt. Contin.* **2**(1), 197–204 (2023).
15. Y. H. Ko et al., "Dual angular tunability of 2D Ge/ZnSe notch filters: analysis, experiments, physics," *Adv. Opt. Mater.* **2022**, 2202390 (2022).
16. J. Song and N. Gupta, "Towards high-performance resonant filter for the long-wave infrared band: fabrication and characterization of notch filters based on the guided mode resonance effect," *Proc. SPIE* **11723**, 11723J (2021).
17. M. G. Moharam et al., "Stable implementation of the rigorous coupled-wave analysis for surface-relief gratings: enhanced transmittance matrix approach," *J. Opt. Soc. Am. A* **12**, 1077–1086 (1995).
18. Y. Matsuoka et al., "Broadband multilayer anti-reflection coating for mid-infrared range from 7 μm to 12 μm," *Appl. Opt.* **57**, 1645–1649 (2018).

Neelam Gupta has a PhD in physics. Currently, she is a research physicist at the Army Research Directorate of the DEVCOM Army Research Laboratory, Adelphi, Maryland, United States. She developed several compact multispectral/hyperspectral imagers from the ultraviolet to the longwave infrared using acousto-optic tunable filters, diffractive optics, MEMS-based filters, etc. She is working on the development of tunable optical notch filters. She is a senior member of Optica, formerly the Optical Society of America.

Junyeob Song received his PhD in electrical engineering from Virginia Tech in 2020, where he studied multiresonant plasmonic cavities. Currently, he is a postdoctoral researcher in the field of nanophotonics. He was a postdoctoral researcher at University of Delaware developing LWIR filters based on guided-mode resonance effect. He is working on developing metasurfaces and integrated nanophotonic systems with semiconductor single quantum dots at the National Institute of Standards and Technology.